Accepted Manuscript

The role of conductive additives on the performance of hybrid carbon xerogels as electrodes in aqueous supercapacitors

María Canal-Rodríguez, J. Angel Menéndez, Miguel A. Montes-Morán, Ignacio Martín-Gullón, José B. Parra, Ana Arenillas

PII: S0013-4686(18)32451-4

DOI: https://doi.org/10.1016/j.electacta.2018.10.189

Reference: EA 32988

To appear in: *Electrochimica Acta*

Received Date: 17 August 2018

Revised Date: 25 October 2018

Accepted Date: 31 October 2018

Please cite this article as: Marí. Canal-Rodríguez, J.A. Menéndez, M.A. Montes-Morán, I. Martín-Gullón, José.B. Parra, A. Arenillas, The role of conductive additives on the performance of hybrid carbon xerogels as electrodes in aqueous supercapacitors, *Electrochimica Acta* (2018), doi: https://doi.org/10.1016/j.electacta.2018.10.189.

THE ROLE OF CONDUCTIVE ADDITIVES ON THE PERFORMANCE OF HYBRID CARBON XEROGELS AS ELECTRODES IN AQUEOUS SUPERCAPACITORS

María Canal-Rodríguez[(a)], J. Angel Menéndez[(a)], Miguel A. Montes-Morán[(a)], Ignacio Martín-Gullón[(b)], José B. Parra[(a)], Ana Arenillas[(a)]*

[(a)]Instituto Nacional del carbón, CSIC, Francisco Pintado Fe, 26, 33011, Oviedo, Spain

[(b)]Chemical Engineering Department, University of Alicante, Apartado 99, 03080, Alicante, Spain

* Corresponding author: Tel. +34985119090, Fax: +34985297662, Email: aapuente@incar.csic.es

ABSTRACT

Three different hybrid carbon xerogels containing Graphene Oxide (AXGO), Micronized Graphite (AXMG) and Carbon Black (AXCB) were synthesized using an easy, fast and affordable method. These three additives were initially selected to improve the electrical conductivity of the pristine activated carbon xerogel (AX) thus expecting to improve its performance in aqueous supercapacitors. Capacitances of the corresponding devices were measured as a function of current density and results of the high and low charge transfer regime of the supercapacitors were discussed separately. In both regimes, the differences observed between the hybrid electrodes were analyzed on the basis of the concurrent influence of the micro and mesoporosity, surface chemistry and electrical conductivity of the materials. Accordingly, even though all the hybrid carbon xerogels showed higher electrical conductivities, only AXGO rendered a better performance than AX, showing the highest capacitances in the whole interval of intensities studied. Consequently, at 16 A g^{-1}, the energy and power densities of the

AXGO supercapacitors increased up to 16% and 97%, respectively, with respect to AX, and of 143% and 409%, respectively, with respect to a commercial activated carbon used as reference. The performance of AXCB and, especially AXMG was worse than AX supercapacitors due to a combination of inadequate pore size distributions and/or a poor surface chemistry. Finally, TEM analysis helped to understand the different way the three additives were affecting the nanostructure (and final properties) of the hybrid carbon xerogels.

Keywords: carbon xerogel, conductive additives, graphene oxide, supercapacitor.

1. Introduction

Due to the current increase in the demand of electrical energy, the development of enhanced energy storage devices that not only store higher amounts of energy, but also modulate the energy demand with a quick response is widely required. Some of the suitable devices that nowadays draw more attention are supercapacitors. These devices are able to combine a high power density supply (up to 10 $kWkg^{-1}$) and long durability (over 10^6 cycles) [1]. Some of the applications where the supercapacitors are catching considerable attention are regenerative braking in the automotive industry, power systems backup and electronic devices [2, 3]. However, their main drawback is their inability to store high energy densities. For that reason, a lot of R&D projects are focused on solving that problem by (i) improving the cell design of supercapacitors [4]; (ii) finding better and more suitable electrolytes [5, 6]; and (iii) developing new electrode materials to store larger amounts of energy. Some of the materials used as electrodes in supercapacitors are metal oxides such as RuO_2 or IrO_2, and conducting polymers [4, 7, 8], both types of materials exhibiting high capacitance and low resistance that result in very high specific power. However, the high manufacturing costs of the first type and the instability that limits the cyclability of the second type

make them non-profitable materials [4, 9]. In consequence, the electrodes most commonly used are made of carbons due to their availability and low cost. In this regard, there are many studies based on improving the properties of carbons to enhance their performance as electrodes for supercapacitors [8, 10-17]. These electrode materials must combine (i) high surface areas (i.e. high micropore volumes) and a certain volume of mesopores of adequate size, (ii) high electrical conductivity and (iii) a suitable surface chemistry. However, obtaining a good combination of all these features is not a straightforward task since high electrical conductivity (typically of ordered carbons) and high surface area (typically of disordered carbons) are usually opposite characteristics. High porosities require discontinuities in the carbon microstructure that difficult the electrons movement, therefore lowering the electrical conductivity. On the contrary, high electrical conductivity is achieved with very condensed and ordered carbon structures, with low defects and consequently low porosity (i.e., low surface area) [18]. Thus, a compromise is normally required.

Moreover, when aqueous electrolytes are used, the surface of the electrode must contain certain amount of oxygen functional groups in order to improve its wettability and the electrode/electrolyte interactions. However, those oxygen species may reduce the electrical conductivity of carbons due to the electronegative character of most of them [19]. It is thus rather difficult to optimize these three properties (i.e. electrical conductivity, adequate porosity and surface chemistry) in a single carbon material.

A possible solution to overcome this problem is to prepare hybrid porous carbons by incorporating a conductive material with a suitable surface chemistry within a porous carbon matrix, in order to facilitate the transport of electrons while retaining the porosity of the matrix [20-24]. Some authors have tried to add graphene, but they found difficulties for dispersing the conductive material in the porous carbon precursor [21].

Other researchers have used graphene oxide suspensions as additive, obtaining the final hybrid material in a subsequent thermal treatment. However, in some cases these materials did not reach sufficiently large pore volumes or their pore size distributions were not optimized for a good diffusion of the electrolyte to supply good energy and power density values. In some others cases, the surface chemistry of the resulting hybrid carbon was not adequate for a good electrode/electrolyte interaction and the final behavior was not as good as expected [21, 24, 25].

In the present study, a graphene oxide, a micronized graphite and a carbon black were used as conductive additives within porous carbon xerogel matrixes. The hybrid additive/organic xerogels were obtained by a fast, easy and affordable method based on microwave heating technology [26]. The final hybrid carbon xerogels were obtained by a thermal treatment. The main aim of this work was to improve the electrical conductivity of the carbon xerogels. Unlike previous studies, the effect of the additives in the performance of the hybrid carbon xerogels as active material for electrodes in supercapacitors was evaluated considering simultaneously the porosity (micro and mesoporosity), electrical conductivity and surface chemistry of the hybrid materials.

2. Experimental

2.1 Synthesis of hybrid carbons

A pristine organic xerogel (OX) was synthesized by the poly-condensation of resorcinol (R) with formaldehyde (F), using water (W) as solvent and a 1M NaOH solution to adjust the pH of the precursor solution. The conditions used were a (R/F) molar ratio of 0.5, a dilution ratio (D) of 5.7 and a pH of 6.5. The precursor solution was heated in a microwave oven during 5 h at 85 ºC where the gelation, curing and drying of the gel took place. A more accurate description of the synthesis of these OXs is reported

elsewhere [27, 28]. It must be highlighted that microwave heating shortens dramatically the synthesis of OXs, which traditionally lasted for several days [29, 30].

Three hybrid organic xerogels were also synthesized using the same conditions as in the case of OX but replacing the synthesis solvent (water) by aqueous suspensions of three conductive additives. The conductive additives used were (i) a commercial Carbon Black (CB) supplied by CABOT, which has very high conductivity and surface area (see supplementary material); ii) a Micronized Graphite (MG) supplied by GARMOR, with much lower porosity than CB (see supplementary information); and (iii) a Graphene Oxide (GO). The aqueous suspensions used were as follows: (i) 5 mg mL^{-1} of CB, (ii) 10 mg mL^{-1} of MG and (iii) 5 mg mL^{-1} of GO. For obtaining OXGO and OXCB the 100 wt% of W was replaced by the aqueous suspensions of GO and CB, respectively. A more detailed description of this process is found in the bibliography [18, 26]. To synthesize OXMG, 50 wt % of the water added for the synthesis was replaced by the aqueous MG suspension mentioned above. The rest of the synthesis conditions were the same as those for OX. Since the dilution factor (D) was fixed to 5.7, this value determined the amount of the additive suspension added during the synthesis. The content of the respective additives in all dried hybrid organic xerogels was thus ca. 0.46 wt%. Given that the maximum temperature reached during the synthesis was 85 ºC, none of the additives were lost during the gelation, curing and drying steps.

The GO suspension was obtained by liquid phase exfoliation through the ultrasonication of graphite oxide according to the modified Hummers-Offeman method employing natural graphite (NG) flakes BNB90 purchased from Imerys Graphite and Carbon (Bodio, Switzerland) [31]. Further details about its production process are given in previous studies [18].

The MG suspension was produced by mixing 10 g of dried MG and 1000 g of deionized water. This mixture was firstly homogenized during 15 min with a magnetic stirrer. Subsequently, the mixture was subjected to two 30-minute ultrasound runs (Bandelin Sonoplus HD 2200) with a power of 200 W.

The CB suspension was made by adding 5 g of CB previously dried in 1000 g of deionized water and the mixture homogenized by stirring during 15 min with a magnetic stirrer. Afterwards, the sample was subjected to ultrasound (Bandelin Sonoplus HD 2200) for 1 h with a power of 200 W.

It is worth to mention, that the homogeneity and stability of the additives suspensions were controlled by leaving the suspension containers without any movement and analyzing the additive content at various heights. Although the additives present different particle size distribution (see Figure S4 in Supplementary Material), the three suspensions were stable and homogeneous during days. Detailed properties of the additives (chemical analysis, physical characterization and electrical conductivity measurements) are shown in the supplementary material.

These pristine and hybrid organic xerogels were used as precursors to obtain activated carbon xerogels, i.e. AX, AXGO, AXMG and AXCB, following a one-step carbonization/activation process in a horizontal oven. The conditions used were 10 g of organic xerogel; CO_2 flow of 50 mL min^{-1}; and a temperature of 1000 ºC with a heating rate of 50 ºC min^{-1}. The dwelling time at the maximum temperature was adjusted to get BET areas of approx. 1600 m^2 g^{-1} for all samples. These dwelling times were very similar for all activation experiments except for AXCB. This sample required 50% longer activation time in order to attain the BET area just mentioned. Nevertheless, it should be pointed out that the activation yield of AXCB was almost identical to the pristine and the rest of the hybrid activated carbon xerogels. In that sense, and assuming

that only (or mainly) the carbon xerogel matrix was being activated during the process, a similar content of additives was expected to remain in all hybrid carbon xerogels (2 wt%).

A commercial activated carbon (YP-50F from Kuraray) specifically designed for its use in supercapacitor electrodes was also included in the present work for comparative purposes.

2.2 Samples characterization

All samples studied were milled and sieved with a sieve of 10 microns before characterization. The textural characteristics of the samples studied were determined on the basis of N_2 adsorption-desorption isotherms recorded at -196 ºC (Micromeritis Tristar 3020). The samples were previously outgassed overnight at 120 ºC at 0.08 mbar of pressure. Parameters such as S_{BET} and V_{micro} were calculated from the Brunauer-Emmett-Teller (BET) and Dubinin-Raduskevich (DR) equations, respectively. Pore size distributions (PSD) were determined by applying NLDFT method to the adsorption branch of the nitrogen isotherm. The total pore volume (V_p) was determined from the amount of nitrogen adsorbed at saturation point (p/p^0= 0.99).

Temperature-programmed desorption (TPD) experiments were performed on a Micromeritics AutoChem II analyzer. The samples were heated up to 1000 ºC at a heating rate of 10 ºC min^{-1} under an Ar flow of 50 mL min^{-1}. The amount of CO and CO_2, desorbed was monitored in a mass spectrometer (OmniStar Pfeiffer).

The micro/nano-metric surface morphology of the materials was examined using high resolution transmission electron microscopy (HRTEM) with a JEOL JEM-2100F microscope operated at 200 kV accelerating voltage. The microscope was equipped with

a field emission gun (FEG) and an ultra-high resolution pole-piece that provided a point-resolution higher than 0.19 nm. The samples were dispersed in ethanol, sonicated and sprayed on a carbon-coated copper grid and then allowed to air-dry.

Particle size distribution of the additives used was performed in a Malvern Mastersizer 3000E, by laser diffraction. The samples were dry analyzed with an Aero-M scatter for powder, at 2 bar and a degree of obscuration between 1-6%.

C and H contents of the additives were measured in a LECO-CHNS-932 microanalyzer, while the O content was determined in a LECO-TF-900 device.

The X-ray photoelectron spectra (XPS) of the additive materials were performed in a SPCS Phoibos 100 analyzer using Mg Kα X-rays (1254.6 eV) programmed to operate at a power of 100W and in a residual vacuum of 10^{-7} Pa. An analyzer with 50 eV pass energy was used to collect the broad scan spectra (0-1100 eV).

To perform the electrochemical characterization of the materials, disc-shaped electrodes were manufactured. The electrodes were prepared by mixing a 90 wt% of each active material with a 10 wt% of polytetrafluoroethylene (PTFE) until getting a homogenous mixture that was rolled out to obtain a thin film. The electrodes were made by punching discs from this film that subsequently were dried and pressed. The resulting electrodes were 100-200 μm thick, 1 cm diameter and 3-5 mg weight. A detailed description of the manufacturing process is available elsewhere [32, 33].

The electrical conductivity of the electrodes was evaluated using the four-point probe technique (FPP) (model SR-4-6L,Ever-being) based on the Van der Pauw equation [33].

The electrochemical measurements were performed by means of a two-electrode testing cell (Teflon Swagelok®) using stainless steel as current collectors where the electrodes were placed, with a glassy fibrous separator (400 μm) and 1 M H_2SO_4 as electrolyte.

The capacitances (C), energy density (E) and power density (P) per active material of a single electrode were calculated from charge-discharge experiments (C-D) at several current densities in the 0.1-16 A g^{-1} range with U= 1 V according to the following expressions [18, 34]:

$$C = 2 \cdot \frac{I}{dV/dt} \qquad (1)$$

Where C is the specific capacitance per active mass of a single electrode (F g^{-1}), I is the current density applied (A g^{-1}) and dV/dt is the slope of the discharge line (V s^{-1}).

$$E = \frac{Ce \cdot [\Delta E]^2}{2 \cdot 3600 \cdot m_e} \qquad (2)$$

$$P = \frac{(\Delta E - \Delta U)^2}{4 \cdot ESR \cdot m_e} \qquad (3)$$

Where Ce is the capacitance of the carbon electrode (F), ΔE is the power-operated window (V), ΔU corresponds to the ohmic fall (V), ESR is the equivalent series resistance (Ω) and m_e is the active mass of the electrode (kg).

Cyclic voltammetry tests were carried out at a scan rate of 2 mV s^{-1} and an electrochemical window between 0.6-1.2 V.

Finally, electrochemical impedance spectroscopy (EIS) analyses were also performed at open circuit (i.e., 0 V) over a frequency range of 1 mHz to 100 kHz and a 10 mV alternating-current amplitude.

3. Results and discussion

Figure 1 shows the variation of the capacitance of the different materials studied, as the current density increases. In general, AXGO was the most stable material showing the highest values of capacitance in the whole range of intensities studied, recording a capacitance drop of less than 30 %. On the other hand, AXMG and AXCB reached capacitances of 112 F g^{-1} at 0.2 A g^{-1}, significantly lower than those of the other samples (ca. 130 F g^{-1}). Also, AXMG and AXCB had poorer capacitance retention than AXGO as the current density increases, in spite of the same quantity of conductive additive added to the three hybrid carbons. In fact, AXCB experienced the same loss of capacitance than AX (40 %) and AXMG similar to that of YP-50F (70 %). The results obtained from Figure 1 will be discussed by dividing the graph in two zones: (i) low current densities (< 1 A g^{-1}) and (ii) high current densities (from 1 to 16 A g^{-1}).

3.1. Low current densities zone

When low current densities are applied, supercapacitors have enough time to charge, i.e. the ions of the electrolyte have sufficient time to get into the micropores of the electrodes [18, 19]. Accordingly, the higher the volume of micropores, the more charge is stored [5, 35]. However, despite the fact that all samples have analogous S_{BET} values (nominally 1600 m^2 g^{-1}), AXMG and AXCB stored 14% less charge than AXGO, AX and YP-50F at 0.2 A g^{-1}. The specific capacitance of supercapacitors at low current densities is a contribution of two main mechanisms [2, 36]: (i) redox reactions due to the presence of certain functional groups on the surface of the electrodes (i.e. the so-called pseudo-capacitance), and (ii) the electrochemical double layer formed at the accessible surface area of the electrodes. The pseudo-capacitance can be caused by the occurrence of oxygen-containing surface groups [5, 6, 16]. These oxygen groups also make the carbon xerogels more hydrophilic materials, improving their wettability and,

therefore, favoring the electrode/electrolyte interactions when using aqueous electrolytes [37-41]. Therefore, good results of capacitance are obtained with a proper combination of a suitable surface chemistry with an adequate micro and mesoporosity [5, 42-44].

Figure 2 shows mainly rectangular voltammograms for all samples, indicating that double layer formation is the main contributor for charge storage. However, (unlike AXCB and AXMG) YP-50F, AXGO and AX also showed a certain contribution of pseudo-capacitance, especially in the case of AX and AXGO as evidenced by the little humps observed at around 0.5 V [16].

Note that in this work all samples were heated at 1000 ºC for several hours. Most oxygenated groups are thus expected to be removed from the carbon surfaces. However, the differences observed in Figure 2 with respect to the performance of the supercapacitors could be ascribed to the different ability of the samples to re-oxidize after the activation/carbonization stage [45]. CO and CO_2 TPD experiments were carried out with all samples (Figure 3). AX was the sample with the highest oxygen content (6.2 wt%) followed by AXGO (4.5 wt%) and YP-50F (3.1 wt%); whereas AXMG and AXCB were the carbons having the lowest oxygen content (2.5 wt% for both carbons). The amount of oxygen-containing surface groups is thus in concordance with the pseudo-capacitive effects observed in the CV plots (Figure 2). The samples with higher amount of oxygen (i.e., AXGO and, especially AX) showed a clearer pseudo-capacitance contribution and therefore higher values of capacitance at low current densities (Figure 1). However, although the oxygen content of AXMG and AXCB is relatively low, it seems hard to credit pseudo-capacitance as being the only responsible for the really different behavior of those two carbons with respect to AXGO and, especially, YP-50F, as shown in Figure 1.

Figure 4 shows the micropore size distributions of all the samples under study. All μPSDs have a maximum at around 0.6 nm. However, significant differences arise when comparing the hybrid xerogels μPSDs with that of the pristine one (AX). AX and AXMG have almost identical micropore size distributions thus suggesting that the addition of MG during the organic xerogel synthesis had little effect on the microporosity of the resulting hybrid carbon xerogel. However, AXCB and AXGO distributions present significant discrepancies with respect to that of AX. AXCB presents a widening of the peak at ca. 0.6 nm that could be attributed to an over-activation of the sample. Actually, higher times of activation (ca. 50 % higher with respect to the other samples studied) were required to get an area of 1600 m^2 g^{-1} in this particular material. In the case of AXGO, its μPSD shows a multi-modal profile with two maximums at ca. 0.6 and 0.9 nm and also a little hump at around 1.7 nm, approximately. This latter feature is also observed to a lesser extent in the distribution of YP-50F (Figure 4).

In accordance with the literature, when aqueous electrolytes are used in supercapacitors the optimum micropore size of the active material should be around 0.7-0.8 nm [5, 6, 14]. Pore sizes below those values seem too narrow for the electrolyte ions to allow the formation of an adequate double layer. This would explain the poor performance of AXMG and AXCB, with most of their micropores having sizes of ca. 0.6 nm. On the contrary, AXGO and YP-50F are the carbons with the highest volume of micropores between 0.7 and 2 nm, with pore volumes of 0.5 and 0.4 cm^3 g^{-1}, respectively. The volumes of pores in the 0.7-2 nm range of AX, AXMG and AXCB is half those values (0.2 cm^3 g^{-1}).Thus, these two carbons would have more volume of micropores fitting the size of the electrolyte ions [42, 43]. It should be highlighted that all samples were activated to have the same BET surface area (i.e. 1600 m^2 g^{-1}). Results obtained would

then confirm that high volumes of micropores of the right size are more relevant than BET surface areas to attain high capacitance values when using activated carbon electrodes [46].

Therefore, considering all factors affecting the charge storage at low current densities (i.e. micropore size distribution, pseudocapacitance, etc.), it can be concluded that the low capacitances achieved by AXMG and AXCB were a consequence of the lack of surface functional groups that would limit their pseudo-capacitance contribution and their wettability, on one hand, and their too narrow micropores that would hinder the access of electrolyte ions to the carbon inner surfaces, on the other. In the case of AX, this latter drawback (narrow micropores) seemed to be compensated by its relatively high surface chemistry. Finally, AXGO and YP-50F would have the best balance of chemical and, especially textural properties (high amounts of micropores of adequate sizes).

3.2. High current densities zone

At high current densities, supercapacitors charge and discharge very rapidly, and there is not enough time to reach all the porosity, especially if there are some constrictions in the structure (i.e. very narrow porosity) [19, 42]. For that reason, to get high capacitances as the current intensity increases, the electrode should have a high micropore volume of the right size, a surface chemistry that favors the wettability and the interaction with the electrolyte and an adequate hierarchical porous structure that eases the access to the microporosity. Thus, to get a fast charge, carbons with a high electrical conductivity and a certain volume of mesopores of appropriate size are required. Mesopores behave as transport pores that enable the movement of the ions when they diffuse towards the micropores. Moreover, the diameter of those mesopores should be wide enough to facilitate the transport of ions [18, 32, 47-49], but keeping in

mind that high mesopore volumes could penalize volumetric capacitance values. Finally, the higher the electrical conductivity, the lower the contact resistance, which enables a fast charge transfer to take place [18, 21, 23, 24]. Finally, the surface chemistry of the electrodes is also an important point to be considered when working at high current densities. In addition to the influence of that chemistry in promoting wettability and/or electrode/electrolyte interactions [19], the electron-withdrawal character of most types of surface oxygen functional groups could reduce the electrical conductivity are opposite characteristics [19, 50].

Returning to Figure 1, the difference between the capacitance values of the samples increased at high current densities. Although all the materials were able to withstand current densities up to 16 A g^{-1}, at these working conditions AXGO rendered the highest capacity (98 F g^{-1}) being 16% and 143% higher than those of AX and YP-50F, respectively. However, AXMG and AXCB showed respectively a capacitance drop of 49% and 21% with respect to the pristine activated carbon xerogel (AX). What is more, AXMG attained the same capacitance as the reference material at 16 A g^{-1} (ca. 40 F g^{-1}). All these differences will be discussed on the basis of the electrical conductivity of the materials, as well as their surface chemistry and textural properties.

Figure 5 shows that all the xerogels have electrical conductivities higher than that of YP-50F (50 S m^{-1}). In fact, the electrical conductivity of AX (110 S m^{-1}) was twice that of the reference material. This higher electrical conductivity is a consequence of the densely packed nanostructure (i.e. structure at the nanometer scale) of the carbon xerogel that favors the electrons mobility through their basic structural units (BSUs), whereas the nanostructure of YP-50F shows some voids or discontinuities that disconnect the carbon platelets or BSUs [18]. As expected, all additives contributed to

increase the electrical conductivity of AX. AXMG rendered the lower enhancement (55%), whereas the electrical conductivity of AXGO almost trebled that of AX (182% increase). The highest electrical conductivity was measured for AXCB (500 S m^{-1}), nearly five times higher than that of AX (355 % increase). This can be attributed to the fact that, unlike GO and MG; carbon black is already a high conductive material that becomes more conductive after the carbonization process of the synthesis of AXCB (see Figure S1). In any case, it is thus expected that the capacitance drop at high current densities of AXCB (Figure 1) would be attenuated by the high electrical conductivity of this material. The performance of YP-50F electrodes, on the other hand, would be strongly hampered at the same working conditions due to their low conductivity.

With respect to the mesoporosity of the samples (Figures 6 and S2), it can be observed that, contrary to the carbon xerogels synthesized, YP-50F is essentially a microporous carbon with very low mesopore volumes (0.2 cm^3 g^{-1}); furthermore, the mesopore size distribution of this material is centered at 2.1 nm, very close to the micropore range. This is an additional drawback that would sum up to the low electrical conductivity of this material to place it as worst performing electrode at high current densities. In the case of AX and AXMG, the mesoPSDs were again almost identical, with mesopore volumes and mesopore average size values of 0.5 cm^3 g^{-1} and 7.0 nm, respectively. This confirms that addition of MG to the organic xerogel did not have any effect on the porosity of the resulting activated carbon xerogel, neither the micro nor the mesoporosity. On the contrary, AXGO shows a broader mesopore size distribution than AX (see Figure 6) with an average mesopore size of ca. 9 nm. This may be due to the fact that the incorporation of GO into the gels structure in AXGO constrained the shrinkage of the organic xerogel during the drying step (see next subsection) [51]. Finally, AXCB was the material with the highest mesopore volume (0.8 cm^3 g^{-1}) and the

widest mesoPSD, centered at 15 nm. This important mesopore contribution in the AXCB PSD is most likely the result of two events: i) CB is a mesoporous carbon (Figure S3) with a mesopore volume and mean pore size of 0.9 cm^3 g^{-1} and 9.5 nm, respectively; and ii) the already mentioned over-activation of this sample would affect both the micro and mesoporosity.

So far, the characterization of the electrical conductivity and mesoporosity of the materials helped to understand the relative electrode performance at 16 A g^{-1} of YP-50F and AXGO with respect to AX (Figure 1). However, two results do not fit the picture: i) AXCB would have been expected to perform much better than observed in terms of stability or low capacitance drop at high current densities due to its very high electrical conductivity and mesoporosity; ii) the AXMG massive capacitance drop when compared to AX at intensive working conditions (i.e., 16 A g^{-1}) is totally unexpected considering the relatively similar electrical conductivities values and identical porosities of both AX and AXMG materials.

In order to clarify this, electrochemical impedance spectroscopy (EIS) analyses were performed. The Nyquist plot (Figure 7) shows that all samples present a 45 º Warburg zone, which means that all electrodes offered certain resistance to the movement of the electrolyte ions through their porous structure. This is related to the equivalent distributed resistance (EDR) of the electrode [52]. AXGO had the less noticeable 45 º Warburg zone and, consequently, the lowest EDR with a value of 0.1 Ω cm^2 (determined from the difference between the linear projection of the vertical portion at low frequencies and the intersection of the 45 º Warburg zone, both on the real axis [4, 16, 52]). The EDR of both AXCB and AX doubled that of AXGO (ca. 0.2 Ω cm^2), whereas the value corresponding to AXMG was much higher, 0.6 Ω cm^2. These values are in accordance with the capacitance drops observed in Figure 1, i.e., AXGO is the

sample with the highest capacitance retention and the lowest EDR, followed by AXCB and AX that have the same capacitance retention and EDR, being AXMG the carbon with the highest capacitance drop and EDR.

As just mentioned, higher values of EDR indicate a poor diffusion of the electrolyte ions into the porosity of the electrode. The high EDR of AXCB when compared to AXGO was certainly unexpected according to the high electrical conductivity and large mesoporosity of the hybrid carbon that contains carbon black. The resistance to the transfer of charge in this sample is thought to be related to the low content of hydrophilic oxygen surface groups (see Figure 3), limiting somehow the interaction of the aqueous electrolyte with the electrode. The role of good electrode wettability (which is here linked to a rich surface chemistry of the material) on its charge storage performance at high current intensities would be even more evident when comparing AX and AXMG. The relatively good stability of AX electrodes (Figure 1) would be a consequence of their rich surface chemistry that would improve electrolyte/electrode interactions especially at high current demand regimes (16 A g^{-1}).

The equivalent series resistance (ESR) of the supercapacitor is determined as the intersection of the loop formed at high frequencies with the real axis in the Nyquist plot (Figure 7) [16]. The ESR value of a given system highly depends on the resistance of the assembly of the supercapacitor cell, which is related to the electrode/current collector contact [18, 53]. AXMG is the sample with the widest high frequency loop, registering an ESR value of 0.9 Ω cm^2. Consequently, the hybrid material with the worse contact (i.e. higher ESR value) is AXMG, followed by AXCB and being AX and AXGO the best samples.

Moreover, the ESR of a cell is also inversely proportional to the power delivered by the supercapacitor, i.e., the higher the ESR, the lower power density will be supplied. The ESR values obtained from the Nyquist plots (Figure 7) are consistent with those calculated from IR drops in the charge-discharge (C-D) tests and, therefore, with the power densities calculated according to equation 3 and shown in the Ragone plot (Figure 8). Since the energy density stored (E) is directly proportional to the capacitance of the electrode (see equation 2), the differences observed between the energy densities of samples in this plot are analogous to the differences of capacitances at 16 A g^{-1} previously analyzed. Accordingly, AXGO is the sample that supplies the highest power density (42000 W kg^{-1}), being the only hybrid material showing a power improvement with respect to both the pristine activated carbon xerogel AX (97%) and the commercial carbon YP-50 F (409%). On the contrary, addition of CB and especially MG downgrades AX performance approaching to power and energy density values close to those of YP-50F (8000 W kg^{-1} and 6 Wh kg^{-1}, respectively).

In short, GO is the unique additive that contributes to obtain a better hybrid carbon xerogel with respect to AX by improving the workability of supercapacitors in terms of energy density (14 Wh kg^{-1}) and power density (42000 W kg^{-1}).

3.3. Integration of additives in the carbon xerogels

In order to understand the effect of the additives on the structural development of the hybrid xerogels hence on their final properties (electrical conductivity, porosity), HRTEM analyses were carried out to make an insight into the structure of the final hybrid samples. Representative images of the samples are shown in (Figure 9).

Images of AXGO (Figure 9) show that the GO is homogeneously distributed and perfectly integrated into the carbon xerogel structure. AXGO is made up of graphene layers embedded in the BSUs of the carbon xerogel [18]. It should be pointed out that

the polymerization reactions of resorcinol (R) and formaldehyde (F) are promoted under acidic conditions. The GO suspension used for the additivation process is strongly acidic (pH < 2) most likely due to residuals of acids used during GO synthesis. This acidic character of GO has been reported to enhance the hydrolysis of cellulose and the dehydration of glucose [54]. Therefore, it is plausible that the GO suspensions also would favor RF polymerization reactions. Furthermore, GO presents many reactive oxygen groups and other structural defects that could also participate in those reactions easing its integration into the carbonaceous structure of the resorcinol-formaldehyde polymer. This good integration of the graphene sheets would improve the electrical conductivity of AXGO (Figure 5) and would reduce the collapse that usually is observed in xerogels during the drying step, showing a higher porosity than the parent xerogel AX, as discussed in the previous subsection (see Figure 6).

The carbon black added to the organic xerogel (OX) to obtain AXCB seems also to have an influence in RF polymerization, but in a different way than GO. In this case, the polymerization seems to occur around CB particles resulting in globular structures that resemble those CB particles (see Figure 9). As a consequence, the characteristic nodules of RF present in the hybrid AXCB materials are bigger than those observed in AX. This would explain the wider mesoporosity of AXCB when compared to AX (Figure 6), since the size of RF nodules determines the space between them (i.e., the mesopores). The connectivity of the CB particles within this hybrid carbon xerogel looks high enough to ensure the boost of the electrical conductivity of the AX pristine material after additivation. Moreover, the high electrical conductivity of AXCB is because the CB particles already have a high electrical conductivity (see supplementary material).

Figure 9 shows very little differences between HRTEM high magnification images of AX and AXMG. It seems that this additive has little effect on the polymerization of the

RF. Consequently, little variations in the porosity are expected after adding MG, as confirmed in the previous subsections (Figures 4 and 6) However, it is worth to remark that at lower magnifications (i.e., 100 and 200 nm scale bars) two different materials are noticed in the HRTEM images of AXMG, indicating the presence of a mixture of two different materials and not a hybrid, as in the other two samples obtained (i.e. AXGO and AXCB). Particles of approx. 100-200 nm size are surrounded by the carbon xerogel nanostructures. These images of AXMG resemble a physical mixture of carbon xerogel and micronized graphite. Particle size distribution of this additive (see Figure S4 in Supplementary Material) shows that the MG sample shows the most wide and heterogeneous particle size distribution, with particles from 0.2 to 90 μm. Whilst CB presents a Gaussian aggregates size distribution and the GO clearly presents aggregates of different sizes, impossible to avoid for the analysis and probably also influenced by the planar nature of GO in comparison to the globular shape of CB. However, these latter samples present “aggregates” of small size (i.e. lower than 20 microns) in comparison to MG. It is also supposed that during the polymerization process in the aqueous media, these aggregates may also be affected and separated. Anyway, the milling and sieving process performed for all the samples studied before characterization (i.e. sieving below 10 microns) may affect big MG particles and/or MG-polymer particles. This makes a difference with GO and CB addition, resulting in a worse connectivity to the polymeric network and thus a very little increase in electrical conductivity of AXMG when compared to AX (Figure 5). The final consequence is the poor behavior of this sample as active material for supercapacitors. However, probably the integration degree of the additives in the RF polymeric structure does not depend on the particles/aggregates size of the additives but more on their surface chemistry and the

ability to participate in the addition and condensation reactions of resorcinol and formaldehyde polymerization.

Therefore, it seems that although initially the three additives used may increase the electrical conductivity of the carbon xerogel, the fact is that there should be a good integration into the polymeric network for this aim. Thus, the additives with low surface oxygen content (Table S1) such as MG and CB do not participate in the polymerization reactions between resorcinol and formaldehyde, and only the GO, with high oxygen content (i.e. 20.1 wt%), may be really integrated into the polymer. This was corroborated by visual validation of different experiments where the additives (i.e. suspensions of GO, CB and MG) were mixed with just one monomer (i.e. resorcinol or formaldehyde) and was subjected to a heating process analogous to the one performed to obtain the hybrid materials. Just in the case of GO it was observed some polymerization reaction between GO-resorcinol and between GO-formaldehyde. On the contrary, MG did not react at all with any of the monomers (i.e., neither resorcinol nor formaldehyde). In the case of CB a kind of intermediate situation was observed. There was no reaction between CB-formaldehyde, but some crystals of resorcinol were observed over the CB after heating at 85ºC. It seems that the globular structure of the CB and its surface chemistry characteristics (i.e. more basic oxygen surface groups than MG, see Table S1) may interact with resorcinol acting as a seed in the polymerization reaction between resorcinol-formaldehyde. The consequence is that this polymerization reaction is favored in the surface of the globular structure of the CB, and thus forming the structures observed in the HRTEM (see Figure 9). The result is a sample with bigger nodules formed by RF polymer around a core of CB. The electrical conductivity of this sample increases a lot, because the CB-core presents a very high conductivity. However, CB is not a good active material in supercapacitor electrodes. Therefore the

final behavior, in terms of farads per gram of sample, of this hybrid sample is notably worse than AX.

The final consequence is that only GO, that it was totally integrated into the polymeric structure increases the properties of an initially good material for supercapacitor such as AX.

4. Conclusions

The synthesis of three hybrid carbon xerogels (AXGO, AXMG and AXCB) containing three different conductive additives (i.e. graphene oxide (GO), micronized graphite (MG) and carbon black (CB)) has shown that not all the additives are incorporated in the same way to the carbon xerogel, and that, therefore, the final hybrid materials have different physical and chemical characteristics. GO is homogeneously distributed through all the carbon xerogel structure. The sheets of graphene reduce the collapse of the xerogel structure that normally takes place during the drying step, rendering a slightly wider mesoporosity and a multimodal micropore size distribution when compared to the pristine activated carbon xerogel (AX). Besides it improves notably its electrical conductivity in a 182 % with respect AX. Moreover, AXGO also has a suitable surface chemistry that improves the electrode/electrolyte interactions. Consequently, AXGO has the most adequate characteristics for this application, providing the highest capacitances at both low current intensities (130 F g^{-1}) and at high ones, with a capacitance drop of less than 30 % of the initial value. Moreover, AXGO shows energy and power densities of 14 Wh kg^{-1} and 42000 W kg^{-1}, respectively. that represent an improvement of 16 and a 97 % with respect to the pristine carbon xerogel

(AX) but a more noticeable improvement of 143 and 409 % with respect to the commercial reference (YP-50F).

Even though CB is also homogeneously dispersed in the carbon xerogel matrix, addition of this additive only improves (very much indeed) the electrical conductivity of the resulting hybrid carbon xerogel (up to ca. 500 S m^{-1}). However, the porosity and more significantly the surface chemistry of AXCB do not favor the electrochemical behavior of this hybrid material as electrode for supercapacitors.

MG is not really integrated into the carbon xerogel structure, i.e., MG does not contribute positively to any feature of the AXMG sample, being the material with the worse behavior as electrode of supercapacitors.

Acknowledgments

Authors gratefully acknowledge the financial support from the Ministerio de Economía, Industria y Competitividad from Spain (Project CTQ2017-87820-R). MCR also acknowledges CSIC (Project I.E. 201880E010).

References

[1] B.E. Conway, Electrochemical supercapacitors: scientific fundamentals and technological applications, Springer Science & Business Media2013.
[2] J. Sánchez-González, F. Stoeckli, T.A. Centeno, The role of the electric conductivity of carbons in the electrochemical capacitor performance, Journal of Electroanalytical Chemistry, 657 (2011) 176-180.
[3] A. Burke, R&D considerations for the performance and application of electrochemical capacitors, Electrochimica Acta, 53 (2007) 1083-1091.
[4] R. Kötz, M. Carlen, Principles and applications of electrochemical capacitors, Electrochimica Acta, 45 (2000) 2483-2498.
[5] V.P. François Béguin , Andrea Balducci , and Elzbieta Frackowiak, Carbons and Electrolytes for Advanced Supercapacitors, Adv Mater, 26 (2014) 2219-2251.
[6] E. Frackowiak, Q. Abbas, F. Béguin, Carbon/carbon supercapacitors, Journal of Energy Chemistry, 22 (2013) 226-240.
[7] S. Ardizzone, G. Fregonara, S. Trasatti, "Inner" and "outer" active surface of RuO2 electrodes, Electrochimica Acta, 35 (1990) 263-267.

[8] P.J. Hall, M. Mirzaeian, S.I. Fletcher, F.B. Sillars, A.J.R. Rennie, G.O. Shitta-Bey, G. Wilson, A. Cruden, R. Carter, Energy storage in electrochemical capacitors: Designing functional materials to improve performance, Energy and Environmental Science, 3 (2010) 1238-1251.
[9] J.P. Zheng, T.R. Jow', P.J. Cygan, Hydrous Ruthenium Oxide as an Electrode Material for Electrochemical Capacitors, Journal of the Electrochemical Society, 142 (1995) 2699-2703.
[10] M. Harmas, T. Thomberg, H. Kurig, T. Romann, A. Janes, E. Lust, Microporous-mesoporous carbons for energy storage synthesized by activation of carbonaceous material by zinc chloride, potassium hydroxide or mixture of them, J Power Sources, 326 (2016) 624-634.
[11] J. Landon, X. Gao, B. Kulengowski, J.K. Neathery, K. Liu, Impact of pore size characteristics on the electrosorption capacity of carbon xerogel electrodes for capacitive deionization, Journal of the Electrochemical Society, 159 (2012) A1861-A1866.
[12] J.-w. Lang, X.-b. Yan, W.-w. Liu, R.-t. Wang, Q.-j. Xue, Influence of nitric acid modification of ordered mesoporous carbon materials on their capacitive performances in different aqueous electrolytes, J Power Sources, 204 (2012) 220-229.
[13] H.M. Lee, L.K. Kwac, K.H. An, S.J. Park, B.J. Kim, Electrochemical behavior of pitch-based activated carbon fibers for electrochemical capacitors, Energy Conversion and Management, 125 (2016) 347-352.
[14] E. Raymundo-Piñero, K. Kierzek, J. Machnikowski, F. Béguin, Relationship between the nanoporous texture of activated carbons and their capacitance properties in different electrolytes, Carbon, 44 (2006) 2498-2507.
[15] P.L. Taberna, P. Simon, J.F. Fauvarque, Electrochemical Characteristics and Impedance Spectroscopy Studies of Carbon-Carbon Supercapacitors, Journal of The Electrochemical Society, 150 (2003) A292.
[16] M. Sevilla, L. Yu, C.O. Ania, M.-M. Titirici, Supercapacitive Behavior of Two Glucose-Derived Microporous Carbons: Direct Pyrolysis versus Hydrothermal Carbonization, ChemElectroChem, 1 (2014) 2138-2145.
[17] G. Lota, T.A. Centeno, E. Frackowiak, F. Stoeckli, Improvement of the structural and chemical properties of a commercial activated carbon for its application in electrochemical capacitors, Electrochimica Acta, 53 (2008) 2210-2216.
[18] M. Canal-Rodríguez, A. Arenillas, N. Rey-Raap, G. Ramos-Fernández, I. Martín-Gullón, J.A. Menéndez, Graphene-doped carbon xerogel combining high electrical conductivity and surface area for optimized aqueous supercapacitors, Carbon, 118 (2017) 291-298.
[19] M. Canal-Rodríguez, J.A. Menéndez, A. Arenillas, Performance of carbon xerogel-graphene hybrids as electrodes in aqueous supercapacitors, Electrochimica Acta, 276 (2018) 28-36.
[20] X.-h. Xia, X.-f. Zhang, S.-q. Yi, H.-b. Liu, Y.-x. Chen, H. Chen, L. Yang, Preparation of high specific surface area composite carbon cryogels from self-assembly of graphene oxide and resorcinol monomers for supercapacitors, Journal of Solid State Electrochemistry, 20 (2016) 1793-1802.
[21] Z. Ling, G. Wang, Q. Dong, B. Qian, M. Zhang, C. Li, J. Qiu, An ionic liquid template approach to graphene-carbon xerogel composites for supercapacitors with enhanced performance, Journal of Materials Chemistry A, 2 (2014) 14329-14333.
[22] F. Meng, X. Zhang, B. Xu, S. Yue, H. Guo, Y. Luo, Alkali-treated graphene oxide as a solid base catalyst: Synthesis and electrochemical capacitance of graphene/carbon composite aerogels, Journal of Materials Chemistry, 21 (2011) 18537-18539.

[23] Z.M. Marković, B.M. Babić, M.D. Dramićanin, I.D. Holclajtner Antunović, V.B. Pavlović, D.B. Peruško, B.M. Todorović Marković, Preparation of highly conductive carbon cryogel based on pristine graphene, Synthetic Metals, 162 (2012) 743-747.
[24] L. Liu, J. Yang, Q. Meng, Graphene cross-linked phenol-formaldehyde hybrid organic and carbon xerogel during ambient pressure drying, Journal of Sol-Gel Science and Technology, 66 (2013) 1-5.
[25] X.H. Xia, X.F. Zhang, S.Q. Yi, H.B. Liu, Y.X. Chen, H. Chen, L. Yang, Y.D. He, Preparation of high specific surface area composite carbon cryogels from self-assembly of graphene oxide and resorcinol monomers for supercapacitors, Journal of Solid State Electrochemistry, 20 (2016) 1793-1802.
[26] J.Ángel Menéndez, Ana Arenillas, Ignacio Martín-Gullón, Gloria Ramos-Fernández. Carbón nanoporoso grafenado, procedimiento de preparación y uso como electrodo Patente Española ES2660884.
[27] E.G. Calvo, N. Ferrera-Lorenzo, J.A. Menéndez, A. Arenillas, Microwave synthesis of micro-mesoporous activated carbon xerogels for high performance supercapacitors, Microporous and Mesoporous Materials, 168 (2013) 206-212.
[28] E.G. Calvo, E.J. Juárez-Pérez, J.A. Menéndez, A. Arenillas, Fast microwave-assisted synthesis of tailored mesoporous carbon xerogels, Journal of Colloid and Interface Science, 357 (2011) 541-547.
[29] L. Liu, G. Tian, R. Ma, G. Pan, W. You, Q. Meng, Preparation and electrosorption performance of graphene xerogel, ECS Solid State Letters, 4 (2015) M9-M11.
[30] K. Zhang, B.T. Ang, L.L. Zhang, X.S. Zhao, J. Wu, Pyrolyzed graphene oxide/resorcinol-formaldehyde resin composites as high-performance supercapacitor electrodes, Journal of Materials Chemistry, 21 (2011) 2663-2670.
[31] I. Rodriguez-Pastor, G. Ramos-Fernandez, H. Varela-Rizo, M. Terrones, I. Martin-Gullon, Towards the understanding of the graphene oxide structure: How to control the formation of humic-and fulvic-like oxidized debris, Carbon, 84 (2015) 299-309.
[32] E.G. Calvo, F. Lufrano, P. Staiti, A. Brigandì, A. Arenillas, J.A. Menéndez, Optimizing the electrochemical performance of aqueous symmetric supercapacitors based on an activated carbon xerogel, J Power Sources, 241 (2013) 776-782.
[33] N. Rey-Raap, E.G. Calvo, J.M. Bermúdez, I. Cameán, A.B. García, J.A. Menéndez, A. Arenillas, An electrical conductivity translator for carbons, Measurement: Journal of the International Measurement Confederation, 56 (2014) 215-218.
[34] T. Brousse, M. Toupin, D. Bélanger, A Hybrid Activated Carbon-Manganese Dioxide Capacitor using a Mild Aqueous Electrolyte, Journal of the Electrochemical Society, 151 (2004).
[35] D. Lozano-Castello, D. Cazorla-Amorós, A. Linares-Solano, S. Shiraishi, H. Kurihara, A. Oya, Influence of pore structure and surface chemistry on electric double layer capacitance in non-aqueous electrolyte, Carbon, 41 (2003) 1765-1775.
[36] T.A. Centeno, F. Stoeckli, The role of textural characteristics and oxygen-containing surface groups in the supercapacitor performances of activated carbons, Electrochimica Acta, 52 (2006) 560-566.
[37] Y.T. Kim, T. Mitani, Competitive effect of carbon nanotubes oxidation on aqueous EDLC performance: Balancing hydrophilicity and conductivity, J Power Sources, 158 (2006) 1517-1522.
[38] C.T. Hsieh, H. Teng, Influence of oxygen treatment on electric double-layer capacitance of activated carbon fabrics, Carbon, 40 (2002) 667-674.

[39] D.-w. Wang, F. Li, M. Liu, H.-m. Cheng, Improved capacitance of SBA-15 templated mesoporous carbons after modification with nitric acid oxidation, New Carbon Materials, 22 (2007) 307-314.
[40] Y.R. Nian, H. Teng, Nitric acid modification of activated carbon electrodes for improvement of electrochemical capacitance, Journal of the Electrochemical Society, 149 (2002) A1008-A1014.
[41] M.J. Bleda-Martínez, J.A. Maciá-Agulló, D. Lozano-Castelló, E. Morallón, D. Cazorla-Amorós, A. Linares-Solano, Role of surface chemistry on electric double layer capacitance of carbon materials, Carbon, 43 (2005) 2677-2684.
[42] A.G. Pandolfo, A.F. Hollenkamp, Carbon properties and their role in supercapacitors, J Power Sources, 157 (2006) 11-27.
[43] C. Lin, J.A. Ritter, B.N. Popov, Development of carbon-metal oxide supercapacitors from sol-gel derived carbon-ruthenium xerogels, Journal of the Electrochemical Society, 146 (1999) 3155-3160.
[44] X. Li, B. Wei, Supercapacitors based on nanostructured carbon, Nano Energy, 2 (2013) 159-173.
[45] J.A. Menéndez, On the use of calorimetric techniques for the characterization of carbons: A brief review, Thermochimica Acta, 312 (1998) 79-86.
[46] B. Lobato, L. Suárez, L. Guardia, T.A. Centeno, Capacitance and surface of carbons in supercapacitors, Carbon, 122 (2017) 434-445.
[47] W. Li, G. Reichenauer, J. Fricke, Carbon aerogels derived from cresol-resorcinol-formaldehyde for supercapacitors, Carbon, 40 (2002) 2955-2959.
[48] E. Frackowiak, G. Lota, J. Machnikowski, C. Vix-Guterl, F. Béguin, Optimisation of supercapacitors using carbons with controlled nanotexture and nitrogen content, Electrochimica Acta, 51 (2006) 2209-2214.
[49] E.G. Calvo, C.O. Ania, L. Zubizarreta, J.A. Menendez, A. Arenillas, Exploring New Routes in the Synthesis of Carbon Xerogels for Their Application in Electric Double-Layer Capacitors, Energy & Fuels, 24 (2010) 3334-3339.
[50] L.R. Radovic, I.F. Silva, J.I. Ume, J.A. Menéndez, C.A.L.Y. Leon, A.W. Scaroni, An experimental and theoretical study of the adsorption of aromatics possessing electron-withdrawing and electron-donating functional groups by chemically modified activated carbons, Carbon, 35 (1997) 1339-1348.
[51] K. Guo, H. Song, X. Chen, X. Du, L. Zhong, Graphene oxide as an anti-shrinkage additive for resorcinol-formaldehyde composite aerogels, Physical Chemistry Chemical Physics, 16 (2014) 11603-11608.
[52] A.B. Fuertes, M. Sevilla, Superior capacitive performance of hydrochar-based porous carbons in aqueous electrolytes, ChemSusChem, 8 (2015) 1049-1057.
[53] Y.R. Nian, H. Teng, Influence of surface oxides on the impedance behavior of carbon-based electrochemical capacitors, Journal of Electroanalytical Chemistry, 540 (2003) 119-127.
[54] F.J. Martín-Jimeno, F. Suárez-García, J.I. Paredes, A. Martínez-Alonso, J.M.D. Tascón, Activated carbon xerogels with a cellular morphology derived from hydrothermally carbonized glucose-graphene oxide hybrids and their performance towards CO2 and dye adsorption, Carbon, 81 (2015) 137-147.

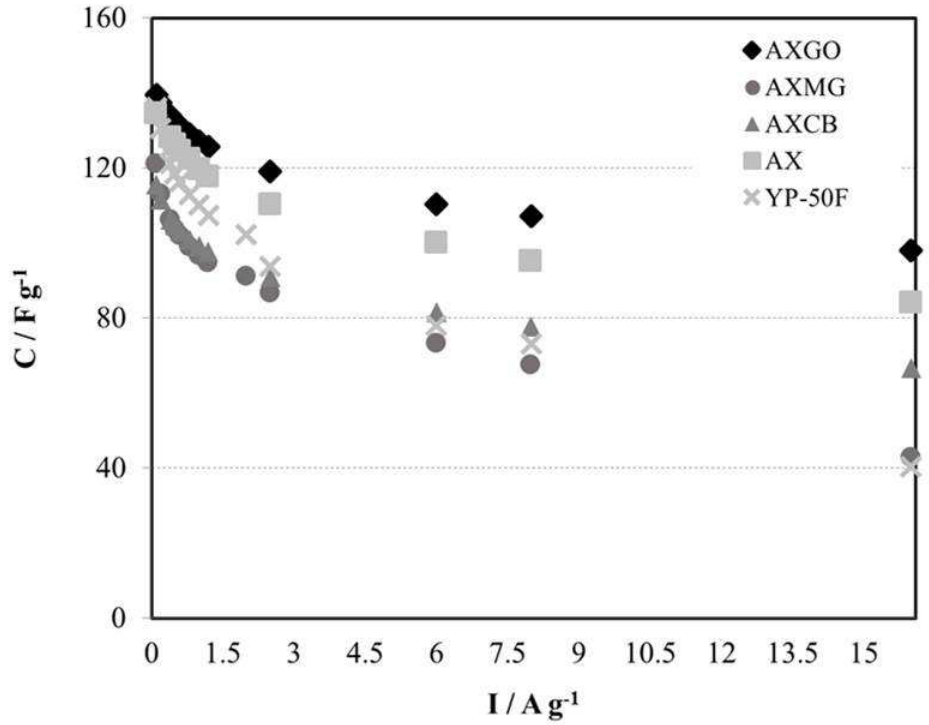

Figure 1. Capacitance values per mass of electrode as a function of current density with U = 1 V of the activated xerogels studied and the reference material

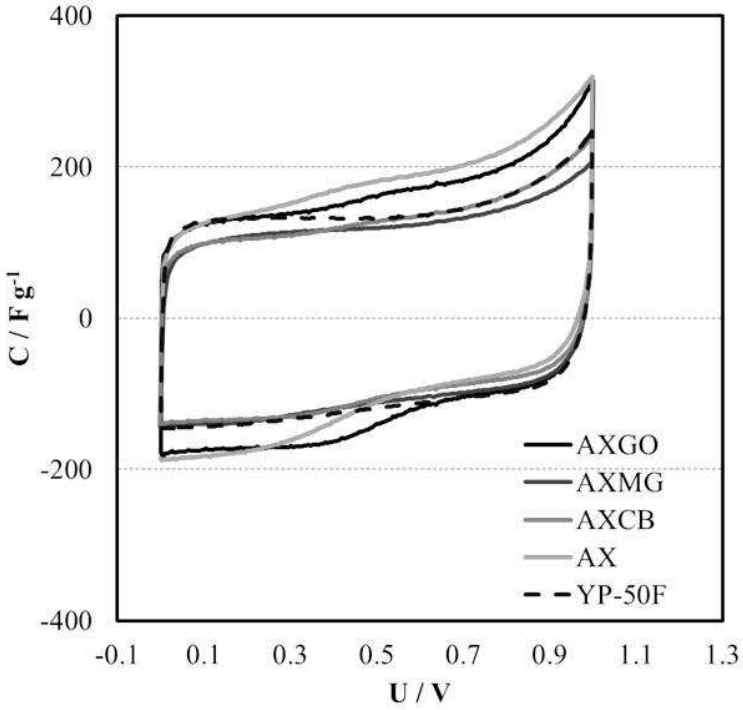

Figure 2. Cyclic voltammetry (CV) curves of the samples studied with a scan rate of 2 mV $s^{-1}$and an electrochemical window of 1 V

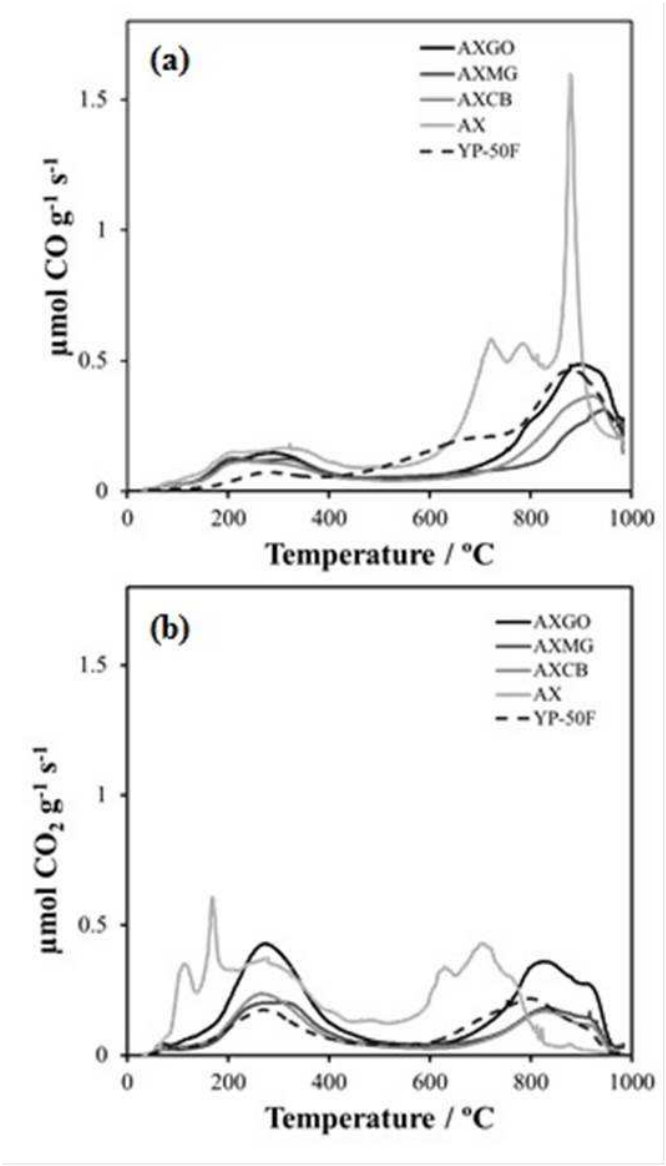

Figure 3. CO (a) and CO_2 (b) desorption profiles of the activated carbon xerogels synthesized and the reference material (YP-50F)

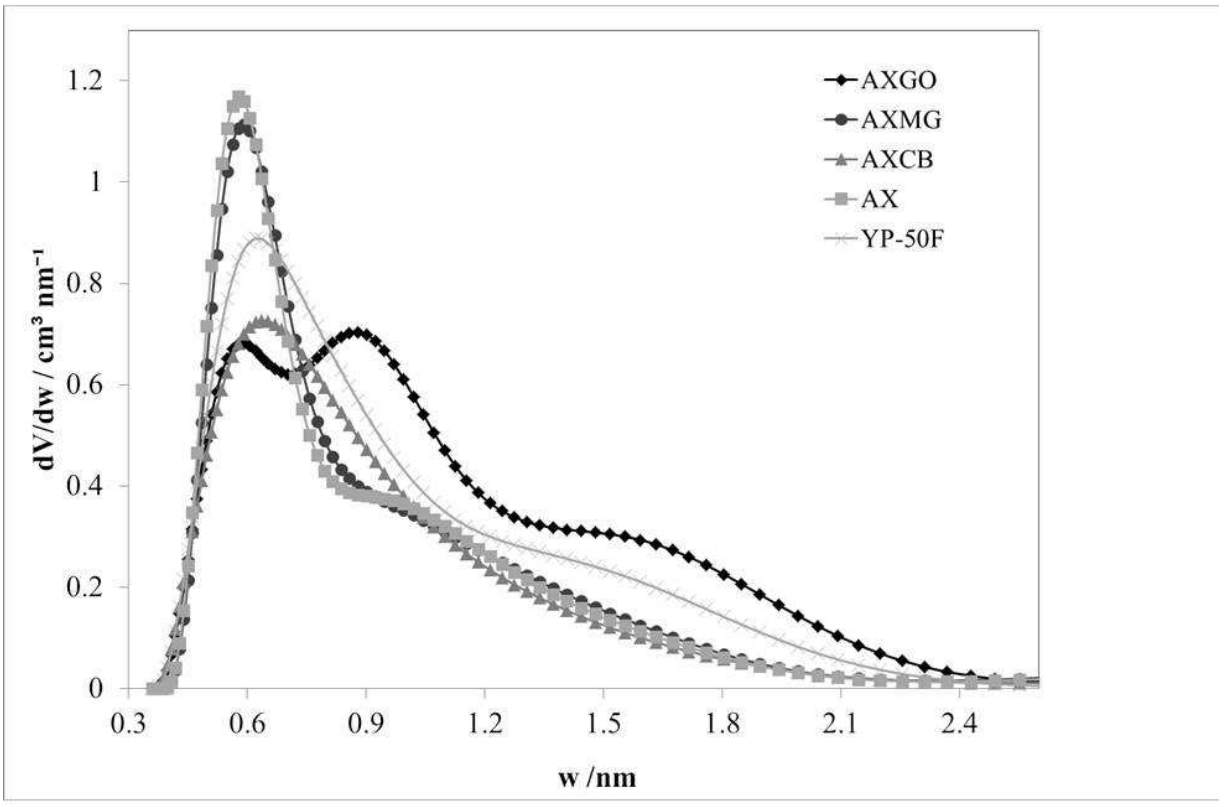

Figure 4. Micropore size distributions of the carbons studied

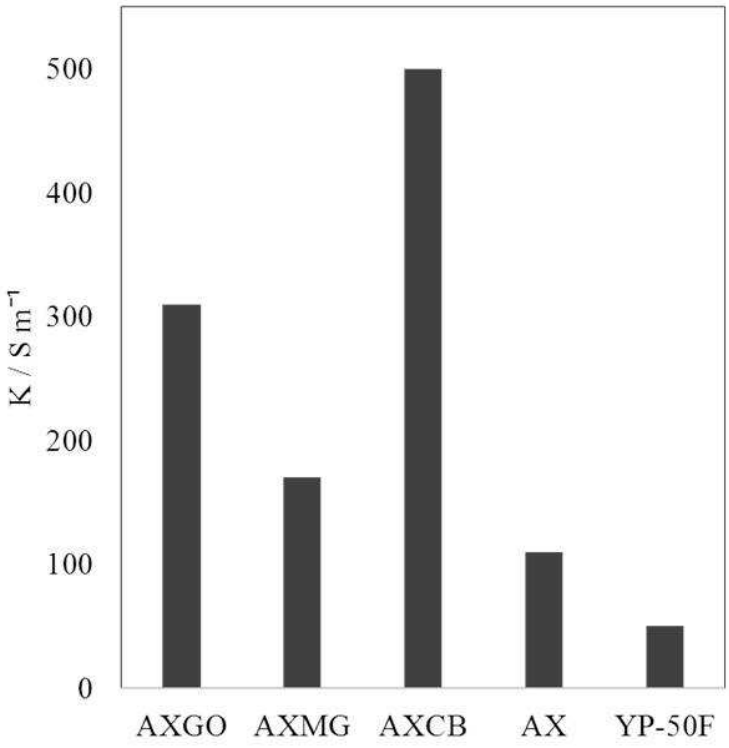

Figure 5. Electrical conductivities of the electrodes made with the carbons studied

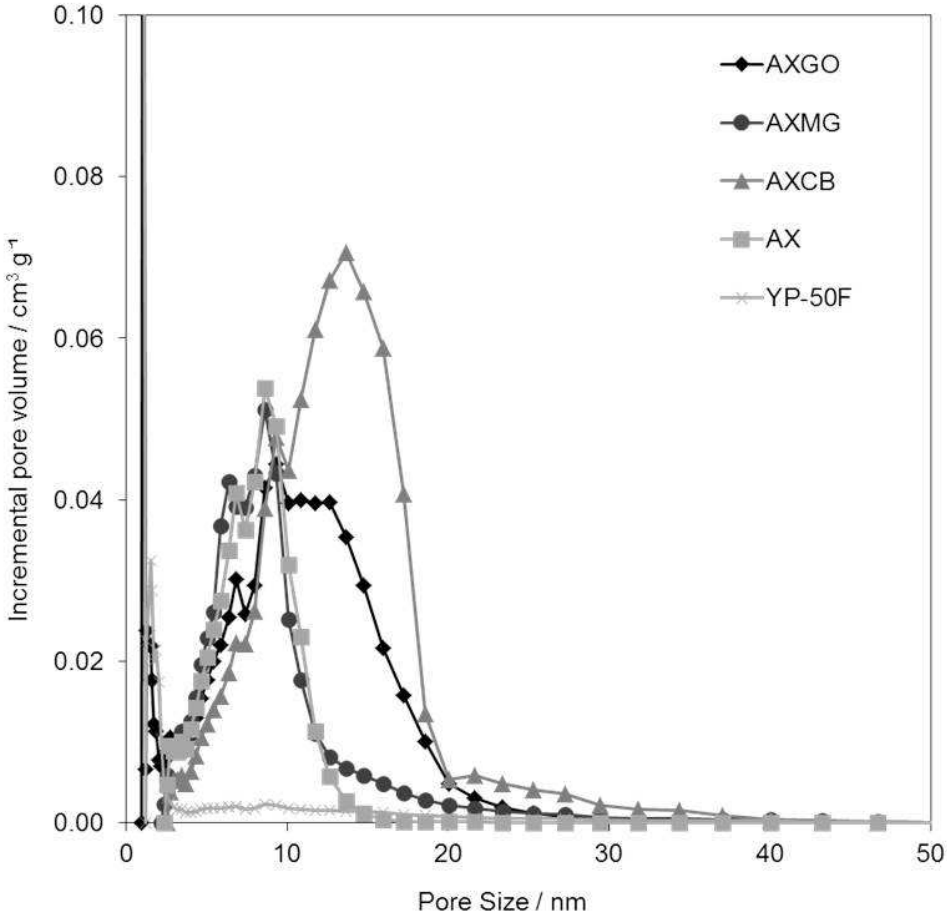

Figure 6. Pore size distributions of the activated carbon xerogels and the reference material

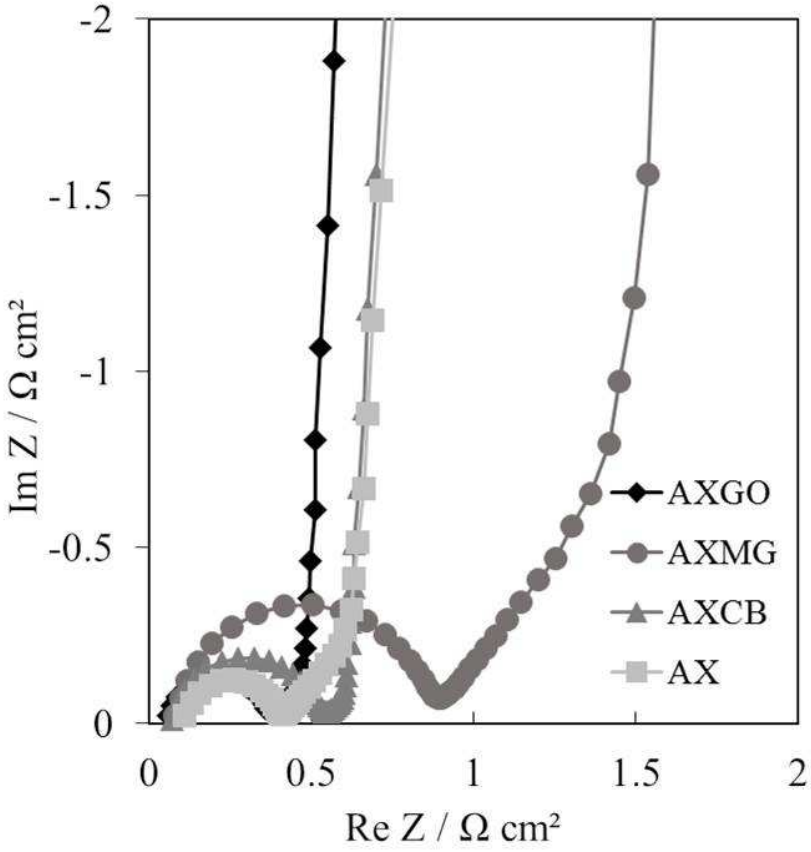

Figure 7. Nyquist plot of the activated carbon xerogels synthesized

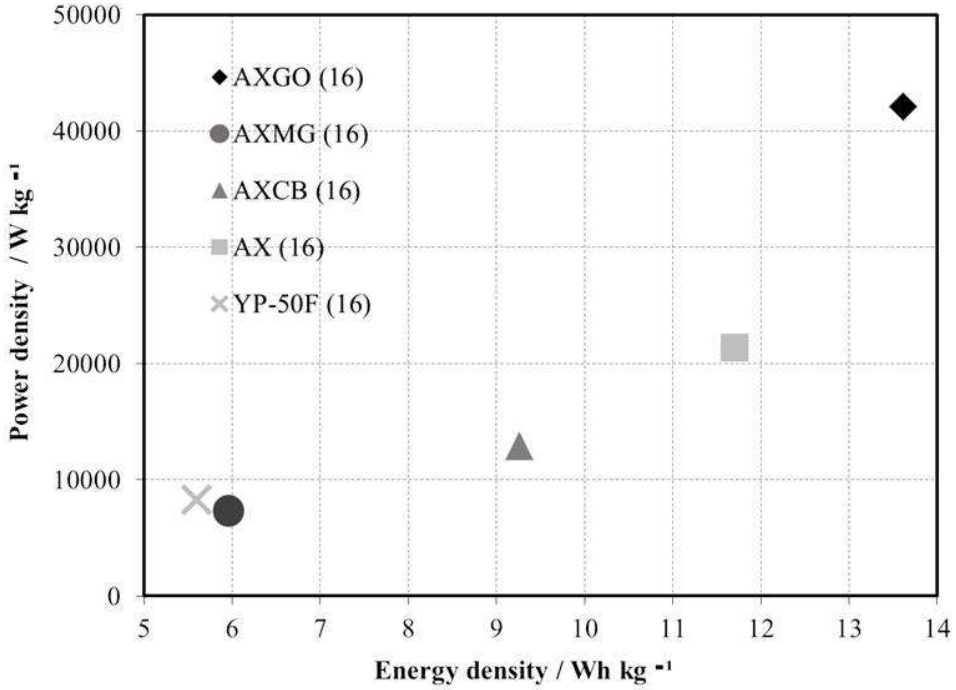

Figure 8. Ragone plot at a current density of 16 A g^{-1} of the samples studied

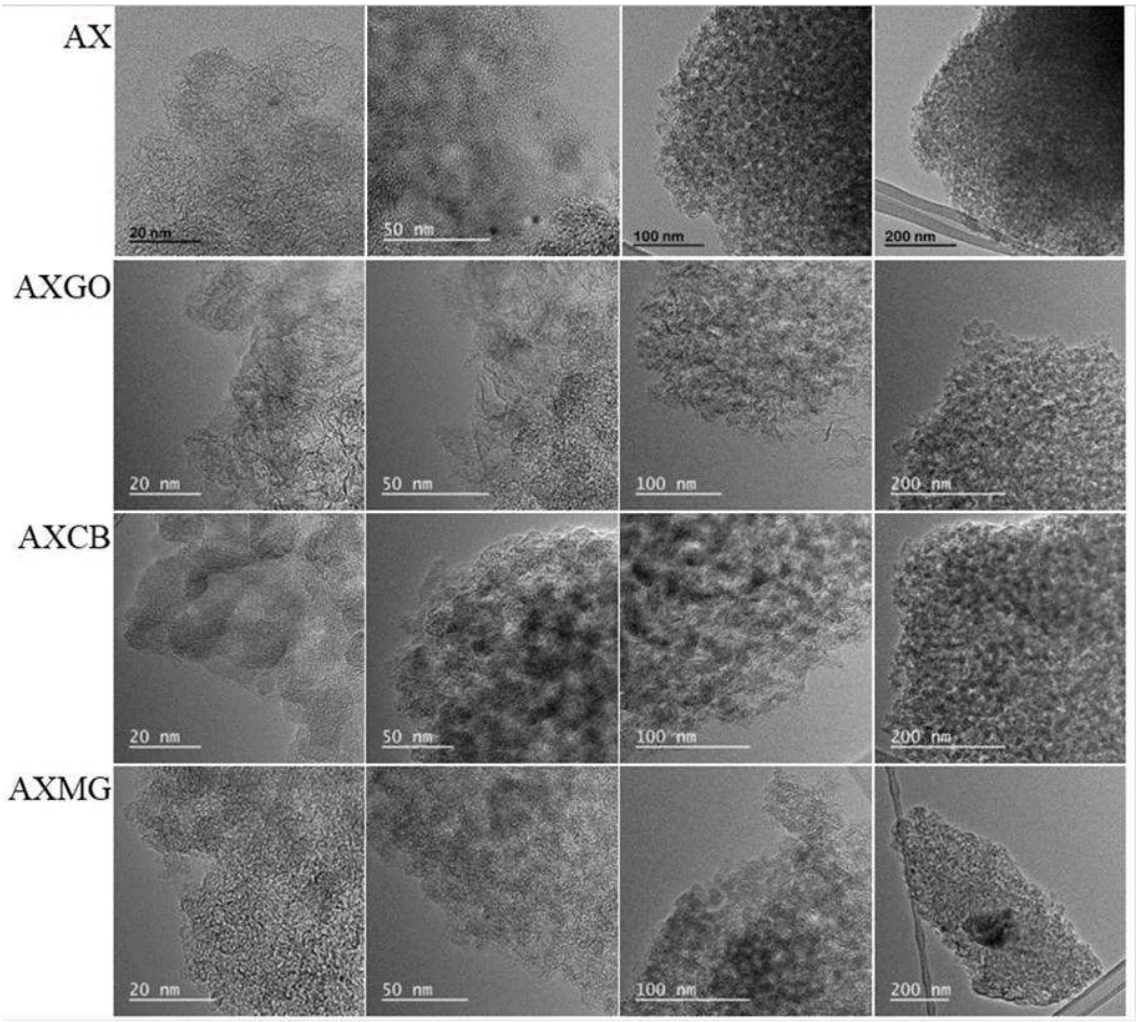

Figure 9. HRTEM images of the hybrid-xerogels and the pristine one

HIGHLIGHTS

- Additive suspensions are incorporated into carbon xerogels during their synthesis
- Electrical conductivity depends on integration of additives into the polymeric structure
- Equilibrium between structure and chemistry in carbons is necessary for electrochemistry
- Graphene oxide seems the best additive for carbon xerogels in electrochemistry